Distinct α-Subunit Structures of Human Insulin Receptor A and B Variants Determine Differences in Tyrosine Kinase Activities†

Monika Kellerer,‡ Rainer Lammers,§ Britta Ermel,‡ Stefanie Tippmer,‡ Beate Vogt,‡ Bert Obermaier-Kusser,‡ Axel Ullrich,§ and Hans-Ulrich Häring*,‡

Institut für Diabetesforschung, Kölner Platz 1, 8000 München 40, Germany, and Max-Planck-Institut für Biochemie, Am Klopferspitz 18a, 8033 Martinsried, Germany

Received June 24, 1991; Revised Manuscript Received December 10, 1991

ABSTRACT: Human insulin receptor isoforms (HIR-A and -B) differ in their α-subunit structures which result from alternatively spliced precursor mRNAs. This structural difference causes distinct binding affinities for insulin. To determine the impact of the structural difference on receptor signaling, we characterized the tyrosine kinase activity of HIR-A and HIR-B in vitro and determined the insulin stimulated β-subunit phosphorylation and tyrosine kinase activation in the intact cell. When ^{32}P incorporation in β-subunits of equal amounts of isolated HIR-A and HIR-B was measured, an increased ^{32}P incorporation in tyrosine residues of the β-subunit of HIR-B (2.5-fold) compared to that of HIR-A was found after in vitro insulin stimulation. This was paralleled by an increased rate of phosphorylation (2.0-fold) of poly(GluNa,Tyr 4:1). In vitro analysis of K_m values for ATP were similar for HIR-A (K_m = 14.3 μM ± 3.8) and HIR-B (K_m = 20.2 μM ± 8.6), whereas the V_{max} of HIR-B was significantly increased (HIR-A V_{max} = 5.5 μmol/60 min μg^{-1} ± 1.4, HIR-B V_{max} = 42.5 μmol/60 min μg^{-1} ± 19.2). HPLC analysis of tryptic β-subunit phosphopeptides revealed identical patterns, suggesting that the difference in kinase activities is not due to an alteration of the phosphorylation–activation cascade within the β-subunit. However, when cleavage of the α-subunit by short-time trypsinization was used to activate the tyrosine kinase, the differences in ^{32}P incorporation between HIR-A and HIR-B were abolished. This suggests that the heterogeneity in the α-subunit structures of HIR-A and HIR-B determines the different kinase activities under basal and insulin-stimulated conditions. To assess whether this difference in kinase activities might be of physiological relevance, we studied receptor autophosphorylation in intact 293 cells transiently overexpressing HIR-A and HIR-B by immunoblotting of the β-subunit with phosphotyrosine antibodies. There was no difference in the receptor autophosphorylation. However, when insulin receptors in intact rat-1 fibroblasts were stimulated with insulin and the receptor was subsequently isolated from the membrane to determine the phosphorylation of poly(GluNa,Tyr 4:1), HIR-B revealed a higher tyrosine kinase activity than HIR-A. These data suggest that HIR-B in solubilized form exists in a conformation that favors tyrosine kinase activation. The physiological significance of this finding, however, remains unknown.

Insulin action at the cellular level is mediated by the insulin receptor in the plasma membrane of target cells (Kahn et al., 1985). The insulin receptor is a heterotetramer consisting of two α-subunits of 135 kDa connected by disulfide bonds to 95-kDa β-subunits which contain a tyrosine kinase activity (Kahn et al., 1985). The insulin receptor subunits are generated by cleavage from a common receptor precursor (Kahn et al., 1985; Yarden & Ullrich, 1988; Ullrich et al., 1985; Ebina et al., 1985). Binding of insulin to the α-subunit of the receptor generates an insulin signal by activation of the intrinsic tyrosine kinase (Kahn et al., 1985), autophosphorylation of the β-subunit (Kasuga et al., 1982, Häring et al., 1984), and subsequent phosphorylation of cellular proteins (White et al., 1985; Häring et al., 1987). Cloning of the insulin receptor DNA revealed the existence of two receptor isoforms which differ in a 12-amino-acid-long sequence in the C-terminal region of the α-subunit (Yarden & Ullrich, 1988; Ullrich et al., 1985; Ebina et al., 1985). This 12-amino-acid insert is encoded by a discrete exon (Seino & Bell, 1989), and it has been shown that alternate splicing gives rise to the two receptor isoforms in a tissue-specific fashion. These two isoforms, termed HIR-A and HIR-B (Yarden & Ullrich, 1988), were expressed in rat-1 fibroblasts. It is known that the binding properties of HIR-A and HIR-B differ (Yarden & Ullrich, 1988; Mosthaf et al., 1990). In the present paper, we study receptor phosphorylation in the intact cell and we describe the isolation of HIR-A and HIR-B from rat-1 fibroblasts and characterization of their tyrosine kinase activity after insulin stimulation in vivo and in vitro. Our experiments demonstrate that HIR-B has a higher tyrosine kinase activity in the basal and the insulin-stimulated state in vitro. Furthermore, our data suggest that the 12-amino-acid insert at the C-terminal end of the α-subunit is functionally important for the interaction of α- and β-subunits and for the control of tyrosine kinase activity.

Materials and Methods

Materials

Plastic material for tissue culture was from FALCON (FRG), DMEM Nutrimix F12 and fetal calf serum were from Gibco (FRG). Porcine insulin was purchased from Novo Industries (Denmark); recombinant human IGF-I[1] and IGF-II

† This work was supported by a grant to H.-U.H. from the Deutsche Forschungsgesellschaft (Ha 1227/3-2) and from the Wilhelm Sander-Stiftung (89.034.1).

* To whom correspondence should be addressed.
‡ Institut für Diabetesforschung.
§ Max-Planck-Institut für Biochemie.

0006-2960/92/0431-4588$03.00/0

were gifts from Chiron Co. (San Francisco, CA) and Eli Lilly Co. (Indianapolis, IN), respectively. [γ-^{32}P]ATP (2900 Ci/mmol) and A14-[^{125}I]monoiodoinsulin were from New England Nuclear (FRG). B26-[^{125}I]monoiodoinsulin and ECL Western blotting detection system were from Amersham International. ^{35}S Tran label was from ICN Biochemicals GmbH. Disuccinimidyl suberate (DSS) was from Boehringer Mannheim (FRG). Trypsin (type VIII), poly(GluNa,Tyr 4:1), aprotinin, and phenylmethanesulfonyl fluoride (PMSF) were from Sigma (St. Louis, MO); wheat germ agglutinin coupled to agarose was from ICN Biomedicals GmbH. Triton X-100, goat anti-rabbit horseradish peroxidase conjugate, and all reagents for sodium dodecyl sulfate–polyacrylamide gel electrophoresis were from Bio-Rad. All other reagents were of the best grade commercially available.

Methods

Cell Culture. Rat-1 fibroblasts transfected either with HIR-A or with HIR-B human insulin receptor type were cultured in DMEM Nutrimix F12 supplemented with 10% fetal calf serum and 200 nM methotrexate in culture plates at 37 °C and 5% CO_2. After they reached confluence, cells were washed 3 times with a Krebs-Ringer–Hepes buffer (pH 7.4) and subsequently removed from culture plates with a rubber polish.

Receptor Preparation. Cells were lysed by freezing and thawing 3 times in the presence of the protease inhibitors phenylmethanesulfonyl fluoride (2.5 mM), aprotinin (1200 trypsin-inhibiting units (TIU/L), leupeptin (2 mM), pepstatin (2 μM), benzamidin (10 mM), bacitracin (0.01%), and leucine (10 mM) in a buffer containing NaH_2PO_4 (pH 7.4, 10 mM), EDTA (5 mM), and sucrose (250 mM). The cell lysate was centrifuged for 50 min at 200000g at 4 °C. The supernatant was discarded, and the pellet was dissolved in a mixture of 25 mM Hepes, 1% Triton X-100, aprotinin (1200 TIU/L), leupeptin (2 μM), pepstatin (2 μM), and phenylmethanesulfonyl fluoride (2.5 mM) and centrifuged for 50 min at 200000g to remove insoluble material. The supernatant was then applied to a column of wheat germ agglutinin coupled to agarose. After being extensively washed with 25 mM Hepes buffer, pH 7.4, containing 0.05% Triton X-100, the bound material was eluted with 25 mM Hepes buffer containing 0.05% Triton X-100 and 0.3 M *N*-acetylglucosamine.

Binding of A14-^{125}I-Insulin to WGA-Purified Receptor. Samples containing 1 μg of solubilized and WGA-purified receptor protein were incubated with 0.0043 nM (20000 cpm) of ^{125}I-insulin and various concentrations of unlabeled insulin for 45 min at 21 °C in a solution containing 50 mM Tris-HCl, pH 7.5, 10 mM $MgSO_4$, and 1% BSA. Separation of the free and receptor-bound insulin was performed by using dextran-coated charcoal (Williams & Turtle, 1979). The amount of ^{125}I-insulin bound to the receptor was determined in a γ-counter, and Scatchard analysis was done with a computer program by G. A. McPherson (McPherson, 1985).

Affinity Cross-Linking of B26-^{125}I-Insulin to WGA-Purified Receptor. Cross-linking experiments were performed as described (Pilch & Czech, 1979; Roth et al., 1986). WGA-purified receptor eluate was incubated with ^{125}I-insulin (0.08–0.1 nM) in the presence or absence of 100 nM unlabeled peptide for 12 h at 4 °C. Tubes were chilled on ice, and 5 μL of DSS (dissolved in dimethyl sulfoxide) was added (final concentration 25 μM) for 20 min at 4 °C. The incubation was terminated by addition of 20 μL of Tris-HCl (200 mM, pH 7.4) and Laemmli buffer containing 100 mM dithiothreitol and by subsequent boiling for 15 min at 95 °C. The reaction products were analyzed by SDS–PAGE (7.5% gel) and autoradiography.

Receptor Phosphorylation. Approximately 1–3 μg of WGA-purified protein was preincubated at 21 °C for 30 min with different concentrations of insulin (0–1000 nM), followed by an incubation with [γ-^{32}P]ATP (10 μCi/μmol) in elution buffer containing 10 mM $MnCl_2$ and 1 mM sodium orthovanadate at 21 °C for 10 min. The incubation was terminated by the addition of Laemmli buffer containing 100 mM dithiothreitol and subsequent boiling for 15 min at 95 °C. The phosphoproteins were separated by 7.5% polyacrylamide gel electrophoresis and identified by autoradiography. Labeled bands were cut out of the gel, and Cerenkov radiation was measured.

Western Blotting. WGA-purified receptor eluate was phosphorylated as described above but without radioactive labeled ATP (unlabeled ATP concentration 5 μM). The phosphoproteins were separated by 7.5% SDS–PAGE and transferred to nitrocellulose by electroblotting. The nitrocellulose was incubated with p-tyr or CT104 antibody, and the bands were detected by a Western blotting detection system (chemoluminescence reaction; ECL, Amersham).

In Vitro Tryptic Activation of WGA-Purified Receptor. Tryptic activation of HIR-A and HIR-B human insulin receptor type was performed as described (Shoelson et al., 1988). Briefly, WGA-purified receptor (1–3 μg of total protein) in 50 mM Hepes, pH 7.4, was incubated with trypsin (type VIII, final concentration 1.5 μM) at 21 °C for 30 s, 60 s, or 5 min. The tryptic digestion was stopped by the addition of PMSF (2 mM) and aprotinin (1 mg/mL). Subsequently, $MnCl_2$ (10 mM), sodium orthovanadate (1 mM), and [γ-^{32}P]ATP (10 μCi) were added for phosphorylation at 21 °C for 10 min. The reaction was terminated by the addition of Laemmli buffer and subsequent boiling for 15 min at 95 °C. Phosphoproteins were separated by SDS–PAGE (7.5% gel).

Substrate Phosphorylation of WGA-Purified Receptor Protein. Substrate phosphorylation activity for kinetic studies was analyzed by a modification of the method of Braun et al. (1984). A total of 0.5–1.5 μg of WGA-purified receptor protein was preincubated with insulin for 30 min at 21 °C. This was followed by an incubation with [γ-^{32}P]ATP (5 μCi) with different concentrations of unlabeled ATP (5–80 μM) in a final volume of 50 μL containing 25 mM Hepes, Triton X-100 (0.05%), 10 mM $MgCl_2$, 10 mM $MnCl_2$, and 1 mM sodium orthovanadate for 10 min. Subsequently, 1 mM poly(GluNa,Tyr 4:1) was added for 1 h (during this time the kinase velocity was linear) at 21 °C. The phosphorylation was stopped by application of the reaction mixture to Whatman 3MM paper squares pretreated by washing with 20 mM sodium pyrophosphate. The samples were washed on paper squares 7 times with 10% trichloroacetic acid containing 20 mM sodium pyrophosphate and counted in an LKB liquid scintillation counter.

Immunoprecipitation. The partially purified receptor protein was immunoprecipitated with the polyclonal insulin receptor antibody B9 at 4 °C for 12 h, and protein A–agarose was added for 2 h at 4 °C. The pellets were washed 3 times with Hepes buffer containing 0.05% Triton X-100. Phosphorylation of the immunoprecipitated receptor was done as described above. Phosphoproteins were identified by autoradiography, and the 95-kDa insulin receptor β-subunit was

[1] Abbreviations: IGF, insulin-like growth factor; WGA, wheat germ agglutinin; DSS, disuccinimidyl suberate; SDS–PAGE, sodium dodecyl sulfate–polyacrylamide gel electrophoresis; BSA, bovine serum albumin; TBS, tris-buffered saline; DTT, dithiothreitol.

excised from the gel and counted in a liquid scintillation counter.

HPLC Tryptic Peptide Mapping. High-performance liquid chromatography was performed as described (Obermaier et al., 1989). Fixed, stained, destained, and dried polyacrylamide gel slices containing the 95-kDa phosphoprotein of HIR-A or HIR-B identified by autoradiography were washed for 24 h at 37 °C with 20 mL of 10% methanol. The gel was dried at 110 °C for 2 h and rehydrated in 600 μL of 50 mM NH_4HCO_3 (pH 8.0) containing 30 μg of L-1-(tosylamino)-2-phenylethyl chloromethyl ketone-treated trypsin (Sigma type VIII). The mixture was incubated for 24 h at 37 °C, the gel fragment was removed, and the supernatant was lyophilized. The residue was dissolved in 50 μL of 0.1% trifluoroacetic acid and freed of particulate material by filtration. The phosphopeptides were separated by using a LKB high-performance liquid chromatography system equipped with a Ultrapac Column TSK ODS-120T (particle size 5 μm). Phosphopeptides applied to the column were eluted at a flow rate of 0.8 mL/min with 0.05% trifluoroacetic acid using a linear acetonitrile gradient from 15% to 25% over 9 min. Fifty fractions of 130 μL were collected, and Cerenkov radiation was measured.

Identification of Phosphoamino Acids. The ^{32}P-labeled β-subunit was identified and trypsin treated as described for HPLC tryptic peptide mapping. After tryptic digestion, phosphopeptides were hydrolyzed in 300 μL of 6 N HCl for 2 h at 110 °C. Each sample was diluted with 2 mL of deionized water, lyophilized, and redissolved in 30–50 μL of water. Electrophoresis was performed on Whatman 3MM paper at pH 3.5 with pyridine/acetic acid/water 10/100/890 (by volume) for 150 min at 1 kV. Phosphoamino acid standards were localized with ninhydrin, ^{32}P-labeled amino acids were localized with autoradiography.

Biosynthetic Labeling of Intact Cells. Subconfluent rat-1 fibroblasts with HIR-A or HIR-B were incubated in a minimal essential medium (MEM) without methionine containing 10% fetal calf serum and 35 μCi/mL Tran ^{35}S label for 30 h at 37 °C. The culture medium was removed, and the adherent cells were washed with a Krebs-Ringer–Hepes buffer (pH 7.4). Subsequently, the cells were removed from the culture plates with a rubber polish and the insulin receptor was isolated as described above.

Transient Expression of HIR-A and B in 293 Cells. The cDNAs for both types of human insulin receptor were cloned into a cytomegalovirus promoter-based expression vector (Gorman et al., 1989), and CsCl gradient purified plasmid DNA was used for transfections. Human embryonic kidney fibroblast 293 cells (ATCC CRL 1573) were grown in DMEM with 10% fetal calf serum, 2 mM L-glutamine, and antibiotics. A total of 3 μg of plasmid DNA for each receptor was transfected into 2×10^5 cells/10 cm^2 well according to the protocol of Chen and Okayama (1987). Eighteen hours after the addition of precipitate, the cells were washed once and supplied with fresh medium containing 0.5% serum; 24 h later the cells were stimulated with insulin for 10 min, the supernatant was aspirated off, and cells were lysed on ice in 0.3 mL of a solution of 50 mM Hepes, pH 7.5, 150 mM NaCl, 1.5 mM $MgCl_2$, 1 mM EGTA, 10% glycerol, 1% Triton X-100, 10 mM sodium pyrophosphate, 100 mM sodium fluoride, 2 mM sodium orthovanadate, 2 mM PMSF, and 10 μg/mL aprotinin. Dishes were incubated for 3 min on ice, and the lysates were collected, kept for 5 min on ice, and centrifuged for 2 min at 13000*g*, from the supernatant lysate receptors immunoprecipitated with mouse monoclonal antibody 83-14

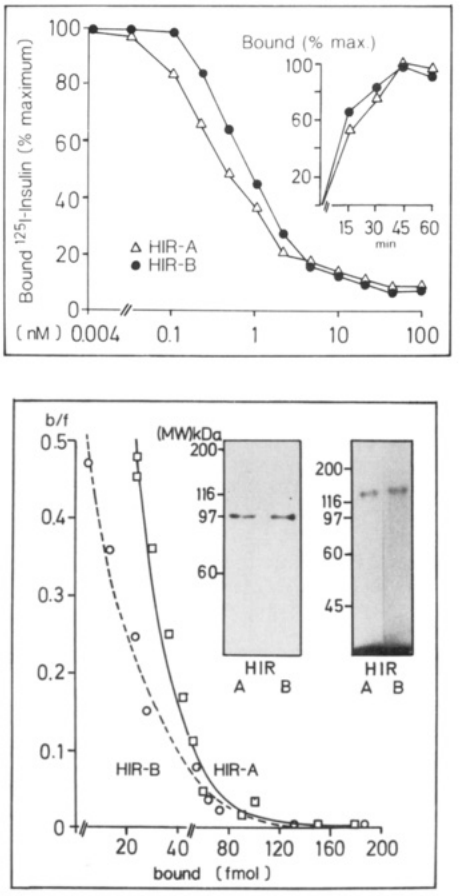

FIGURE 1: (Top) Representative displacement curve of A14-^{125}I-insulin binding to HIR-A and HIR-B. The WGA-purified insulin receptor was incubated with ^{125}I-insulin and increasing concentrations of unlabeled insulin for 45 min at 21 °C. Under these conditions, binding was at equilibrium (insert of the top panel). Binding of ^{125}I-insulin is expressed as the percentage of maximum binding obtained in the absence of unlabeled insulin. (Bottom) Representative Scatchard plot of the binding of ^{125}I-insulin to HIR-A and HIR-B. Binding was measured as described above. Scatchard analysis was done with a computer program by G. A. McPherson (1985). The same receptor amount was controlled by Western blotting. The left insert shows the result of an immunoblot with the β-subunit antibody CT104. The samples were applied to a 7.5% SDS–PAGE in the presence of 100 mM DTT. Proteins were transferred to nitrocellulose, and the nitrocellulose was incubated with the polyclonal CT104 antibody. The right insert of the bottom panel shows the autoradiogram from the cross-linked α-subunit of the insulin receptor. Receptor amounts of HIR-A and HIR-B were identical to the receptor number used for binding data and Scatchard analysis in panel B. The 135-kDa α-subunit of the insulin receptor was cross-linked to ^{125}I-insulin with DSS, and the labeled bands were separated by 7.5% SDS–PAGE. The 135-kDa bands were cut out of the gel and counted in a γ-counter (HIR-A, 5400 cpm; HIR-B, 4050 cpm).

(Soos et al., 1986) and 20 μL of protein A–Sepharose slurry (1/1, swollen and prewashed in lysis buffer). The immunoprecipitates were washed once in lysis buffer and boiled with Laemmli buffer, and proteins were analyzed by electrophoresis on 7% SDS–polyacrylamide gels. For immunoblotting, proteins were transferred electrophoretically to nitrocellulose, first probed with anti-phosphotyrosine mouse monoclonal antibody 5E.2 (Fendley et al., 1990) and the ECL system of Amersham Corp. and then stripped by incubation for 1 h in a mixture of 150 mM glycine and 100 mM NaCl and reprobed with polyclonal antibody CT104 against a carboxy-terminal peptide (amino acids 1327–1343 of HIR-A) of the insulin receptor.

RESULTS

Binding Properties of Partially Purified Receptor and Standardization of Receptor Number. Insulin receptors were

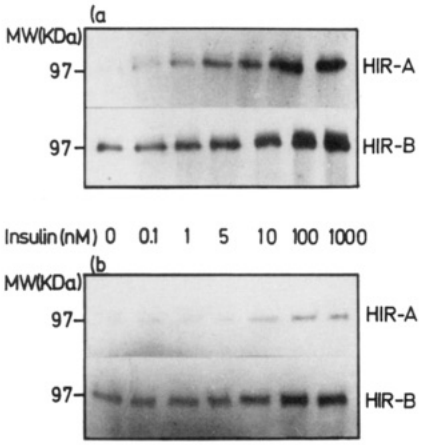

FIGURE 2: Autoradiograms showing phosphorylation of the 95-kDa insulin receptor β-subunit of HIR-A and HIR-B. Panel a shows the ^{32}P incorporation after the same amount of WGA-purified protein of HIR-A and HIR-B was used. Panel b shows the ^{32}P incorporation after the same receptor amounts were used as determined by the Scatchard analysis and controlled by two different methods. Samples were incubated with different insulin concentrations (0–1000 nM) for 30 min and phosphorylated as described in the Methods section for 10 min, stopped, and then applied to SDS–PAGE (7.5% gel).

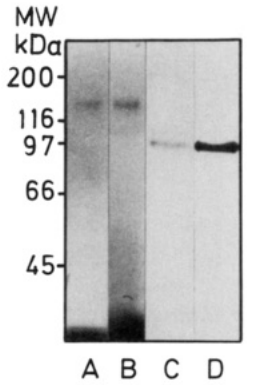

FIGURE 3: Comparison of cross-linking of ^{125}I-insulin and autophosphorylation of HIR-A and HIR-B. ^{125}I-Insulin (0.1 nM) was chemically cross-linked to the WGA-purified HIR-A and HIR-B with 25 μM DSS. The ^{125}I-labeled α-subunit is shown on the left side of the figure (lane A, HIR-A 857 cpm; lane B, HIR-B 884 cpm). The same receptor amounts were used for autophosphorylation in the presence of 0.1 nM unlabeled insulin at 21 °C for 30 min. Subsequently, [γ-^{32}P]ATP was added for 10 min at 21 °C. The reaction was stopped and applied to 7.5% SDS–PAGE as described in the Methods section (lane C, HIR-A 654 cpm; lane D, HIR-B 2271 cpm).

isolated from transfected rat-1 fibroblasts as described in the Methods section, and their binding properties were determined under equilibrium conditions (see the insert in the top panel of Figure 1). The top panel of Figure 1 shows a representative displacement curve of the binding data of WGA-purified insulin receptors. As described earlier (Mosthaf et al., 1990), A- and B-receptors differ with respect to insulin affinity (half-maximal inhibition of binding: HIR-A, 0.5 nM; HIR-B, 0.8 nM insulin). The bottom panel of Figure 1 shows a Scatchard plot after dilution to the same receptor amounts as determined from a previous Scatchard plot with same amounts of WGA-purified protein. Both receptors reveal a curvilinear Scatchard plot. A-receptors displayed a higher affinity for insulin than B-receptors. These data confirm in general the previously reported binding characteristics of HIR-A and HIR-B (Mosthaf et al. 1990). To further characterize the binding properties, we determined the relative affinity of IGF-I and IGF-II to both receptor types. The typical hierarchy of the affinities of these peptide hormones, i.e., insulin > IGF-II > IGF-I (Van Wyk et al., 1980; Kasuga et al., 1981), was found for both receptor types (data not shown).

In order to compare the kinase activities of HIR-A and HIR-B in vitro, the partially purified receptor preparations were diluted to yield the same amounts of receptors. Dilution was done on the basis of the binding data and was controlled by chemical cross-linking with ^{125}I-insulin to the α-subunit (bottom panel of Figure 1, right insert, α-subunit labeling: HIR-A, 5400 cpm; HIR-B, 4050 cpm) and by immunoblotting with an antibody against the β-subunit (bottom panel of Figure 1, left insert, scanning densitometric analysis (total absorption: HIR-A, 626; HIR-B, 713). The inserts of the bottom panel of Figures 1 show that dilution on the basis of Scatchard plots reveals comparable amounts of cross-linked or immunoblotted receptors.

Basal and Insulin-Stimulated Autophosphorylation of Partially Purified Insulin Receptor. Figure 2 shows autoradiograms of basal and dose-dependent insulin-stimulated autophosphorylation of the 95-kDa β-subunit at equilibrium. Equilibrium autophosphorylation was reached with the same time course in HIR-A and HIR-B (data not shown). First, ^{32}P incorporation was measured using (a) equal amounts of wheat germ lectin purified proteins. The ^{32}P incorporation in these bands was measured, and the ratio HIR-B/HIR-A was 4.3-fold (n = 4) under basal conditions and 3.8-fold (n = 4) under insulin stimulation. If wheat germ proteins were diluted to yield the same amounts of receptors (b) as determined by Scatchard analysis and controlled as described in the preceding paragraph, the factor HIR-B/HIR-A was 2.4-fold (n = 7) under basal conditions and 2.5-fold (n = 7) under insulin stimulation. In addition, type A and B receptors were compared by cross-linking of the α-subunit with 0.1 nM ^{125}I-insulin and by autophosphorylation at the same concentration (0.1 nM) of unlabeled insulin (Figure 3). While similar levels of cross-linking were seen, a clear difference for ^{32}P incorporation is evident. Furthermore, we labeled rat-1 fibroblasts with [^{35}S]methionine for 30 h. The ^{35}S-labeled insulin receptor was isolated and partially purified by a WGA column. To quantify the ^{35}S incorporation into the 95-kDa band, receptors were separated on an 7.5% SDS–polyacrylamide gel and the radioactive incorporation was determined by cutting out the 95-kDa band from the dried gel and by counting the radioactivity in a liquid scintillation counter. The ^{35}S incorporation was clearly increased in HIR-B, which might be a consequence of the increased receptor number in these cells compared to fibroblasts transfected with HIR-A (^{35}S incorporation: HIR-A, 242 cpm; HIR-B, 1176 cpm). In parallel, the ^{35}S-labeled receptor was autophosphorylated with [γ-^{32}P]ATP and 100 nM insulin. The 95-kDa bands were cut out of the gel, and the ^{32}P incorporation into these bands was determined (HIR-A, 186 cpm; HIR-B, 4106 cpm). The ratio of $^{32}P/^{35}S$ incorporation was calculated. For HIR-A, a ratio of $^{32}P/^{35}S$ incorporation of 0.77 was found; for HIR-B, the ratio was 3.49. This suggests a higher level of ^{32}P incorporation per ^{35}S incorporation in HIR-B compared to in HIR-A.

Poly(GluNa,Tyr) Phosphorylation after in Vitro Insulin Stimulation of HIR-A and HIR-B. The kinase activity of HIR-A and HIR-B against the synthetic substrate poly-(GluNa,Tyr 4:1) was determined as described in the Methods section. WGA-purified HIR-A and HIR-B were normalized on the basis of Scatchard plots. The kinase activity without insulin stimulation was 192 231 cpm for HIR-A and 459 755 cpm for HIR-B (counts per minute per 150 fmol of receptor). After insulin stimulation in vitro, 313 669 cpm were measured in HIR-A and 638 927 cpm were measured in HIR-B (mean

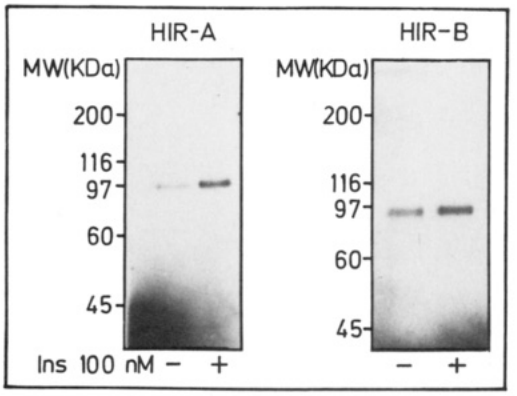

FIGURE 4: Autoradiograms showing the immunoprecipitated and phosphorylated insulin receptor β-subunit from HIR-A and HIR-B. Both HIR-A and HIR-B were adjusted to equal amounts of receptors as determined by Scatchard analysis. As described in the Methods section, the insulin receptors were incubated with the polyclonal receptor antibody B9. The immunoprecipitates were washed 3 times with Hepes buffer containing 0.05% Triton X-100 and subsequently incubated in the absence (−) and presence (+) of 100 nM insulin. The samples were phosphorylated with [γ-^{32}P]ATP for 10 min, stopped, and then applied to 7.5% SDS–PAGE. Phosphoproteins were identified by autoradiography. The 95-kDa bands were excised from the dried gel, and the radioactivity was measured in a liquid scintillation counter.

values of two separate experiments performed in duplicate). Thus, substrate phosphorylation shows a difference for HIR-A and HIR-B similar to autophosphorylation.

Determination of Phosphoamino Acids. To determine whether the differences in autophosphorylation were due to an inhibition of A-receptors by a serine kinase activity, which may contaminate WGA–insulin receptor preparations and might phosphorylate the receptor at serine residues, we characterized the phosphoamino acid composition of the autophosphorylated β-subunit. The phosphoamino acid analysis of both HIR-A and HIR-B showed that only tyrosine residues were phosphorylated in vitro (data not shown). Thus, no evidence could be found for the presence of a potentially inhibiting serine kinase in the phosphorylation assay.

Autophosphorylation of HIR-A and HIR-B Receptors after Immunoprecipitation. To test the possibility that regulatory proteins other than serine kinases are responsible for the lower activity of HIR-A, we studied receptor autophosphorylation after immunoprecipitation of insulin receptors with the polyclonal insulin receptor antibody B9 (Figure 4). WGA-purified preparations were adjusted to equal amounts of insulin receptors on the basis of the binding studies and were then immunoprecipitated with antibody B9. The precipitates were extensively washed, and autophosphorylation under basal and insulin-stimulated conditions was measured for HIR-A and HIR-B. The same ratio as described above was found for ^{32}P incorporation in the β-subunits of both receptor types (for basal, HIR-A 329 cpm and HIR-B 633 cpm; for insulin stimulated, HIR-A 785 cpm, HIR-B 1678 cpm). This suggests that the difference between HIR-A and HIR-B kinase activities is intrinsic to the receptor itself rather than a function of loosely associated regulatory proteins. However, the presence of a more tightly associated protein like, for example, PI-3 kinase cannot be excluded.

Determination of the Kinetic Enzyme Constants of HIR-A and HIR-B. To determine whether the differences in kinase activity were due to an alteration of the K_m for ATP, we studied phosphorylation of the exogenous substrate poly(GluNa,Tyr 4:1) at different ATP concentrations. The Lineweaver–Burk plot (data not shown) revealed no significant difference in the K_m for ATP of both receptors [HIR-A, K_m = 14.3 μM ± 3.8 (n = 4); HIR-B, K_m = 20.2 μM ± 8.6 (n = 4)]; however, a clear difference in V_{max} (micromoles per 60 min per microgram of WGA-purified protein) [HIR-A, V_{max} = 5.5 ± 1.4 (n = 4); HIR-B, V_{max} = 42.5 ± 19.2 (n = 4)] was seen under insulin-stimulated conditions. The unaltered K_m for ATP is consistent with the phosphoamino acid studies of HIR-A and HIR-B showing no serine phosphorylation, since we had previously observed (Häring et al., 1986a,b) that the inhibitory mechanism caused by serine phosphorylation is associated with an increased K_m for ATP. Thus, not only serine phosphorylation of HIR-A during the in vitro assay but also an increased prephosphorylation of HIR-A at serine residues in the intact cell is unlikely to be the cause of the different kinase activities.

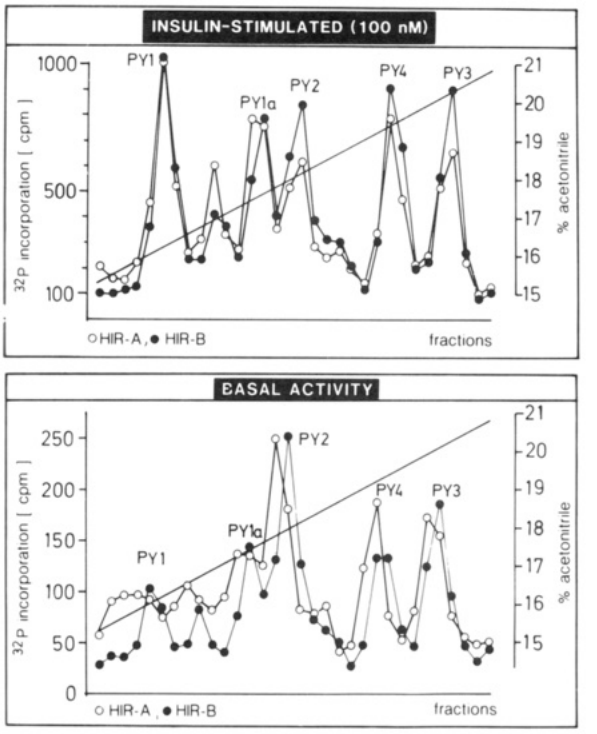

FIGURE 5: HPLC tryptic phosphopeptide mapping of the 95-kDa β-subunit of HIR-A and HIR-B. WGA-purified receptors were phosphorylated under basal and insulin-stimulated conditions and prepared for HPLC phosphopeptide mapping as described in the Methods section. Equal radioactivity of HIR-A and HIR-B was applied to the HPLC column. Fractions of 130 μL were collected, and Cerenkov radiation was measured.

Characterization of the Tryptic Peptide Maps of the Phosphorylated Receptor β-Subunits by HPLC. In order to determine whether the different kinase activities could be attributed to differences in the so-called autophosphorylation cascade (White et al., 1988), we performed a tryptic digestion of phosphorylated receptor β-subunits and separated the phosphopeptides by HPLC as described (White et al., 1984, 1988; Obermaier et al., 1989). As reported earlier, ^{32}P incorporation occurs predominantly in peptides containing tyrosine 1146, 1150, and 1151 or 1158, 1162, and 1163, respectively termed pY1, pY1A (triphosphorylated form), and pY4 (diphosphorylated form). Furthermore, C-terminal phosphorylation sites can be separated (pY2 and pY3). Figure 5 shows the tryptic peptide profile under basal conditions and maximal insulin stimulation for both receptor types. For comparison, equal amounts of radioactivity were applied to the column. There was no significant difference in the relative distribution of the phosphopeptides detectable between both receptor types either in the basal state or in the insulin-stimulated state. In both receptors, a comparable increase of the

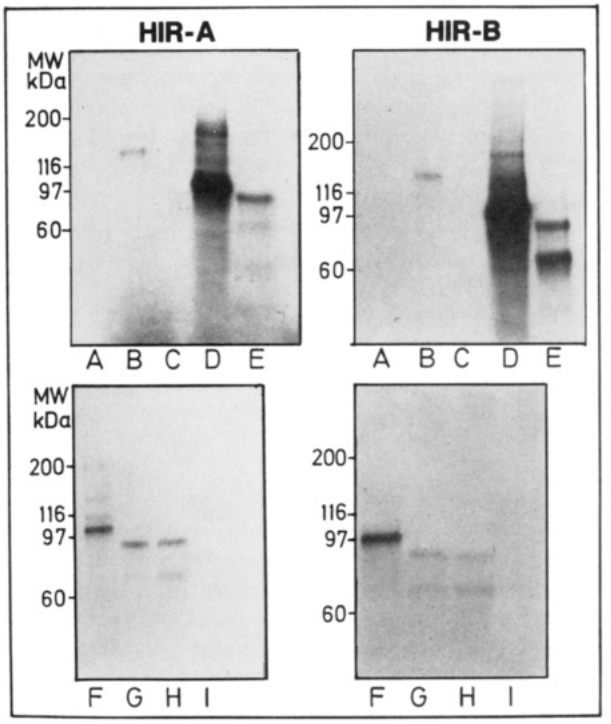

FIGURE 6: (Upper panel) Autoradiograms of HIR-A and HIR-B showing a comparison of α-subunit labeling, autophosphorylation, and tryptic activation in a single gel using comparable amounts of insulin receptors as determined by Scatchard analysis and by labeling of the α-subunit. Specificity of ^{125}I-insulin binding to the α-subunit (α-subunit labeling: HIR-A, 1591 cpm; HIR-B, 1528 cpm) is shown in the presence (lane A) and absence (lane B) of unlabeled insulin (100 nM). Another cross-linking experiment was done after treatment with 1.5 μM trypsin for 30 s (lane C). The same amount of insulin receptor as in the cross-linking experiments was used for autophosphorylation stimulated either with 100 nM insulin (lane D) or by cleavage of the α-subunit with 1.5 μM trypsin for 30 s (lane E). Bands were excised from the dried gel, and the radioactivity was measured in a liquid scintillation counter. (Lower panel) Comparison of tryptic activation kinetics of HIR-A and HIR-B: lane F, insulin-stimulated autophosphorylation (100 nM insulin); lane G; trypsin-stimulated autophosphorylation at 30 s; lane H, trypsin-stimulated autophosphorylation at 1 min; lane I, trypsin-stimulated autophosphorylation at 5 min.

triphosphorylated peptide PY1 and pY1a occurred after insulin stimulation.

Effect of Trypsin on Receptor Autophosphorylation. In order to elucidate whether the different kinase activities were due to the differences in HIR-A and HIR-B α-subunit structure or they were intrinsic to the β-subunits, we tested the effect of trypsin on kinase activation. Short-time trypsinization of solubilized insulin receptors is a method to activate the intrinsic tyrosine kinase activity of the insulin receptor independent of insulin (Shoelson et al., 1988). Under these conditions, a cleavage of the α-subunit of the insulin receptor occurs, which leads to activation of β-subunit autophosphorylation (Shoelson et al., 1988). The autoradiograms in lower panel of Figure 6 show the effect of trypsinization for 30 s (lane G), 1 min (lane H), and 5 minutes (lane I). After 30 s, the stimulated receptor β-subunit migrates as an 80-kDa band on autoradiograms, but also a 60-kDa band appears predominantly in HIR-B after 30 s and at 1 min also in HIR-A (lane H). These phosphoproteins (pp80 + pp60) are no longer detectable after a trypsinization time of 5 min (lanes I).

To compare the trypsin-activated intrinsic kinase activity of HIR-A and HIR-B, WGA-purified proteins were divided into two aliquots. The first aliquot was used to label the

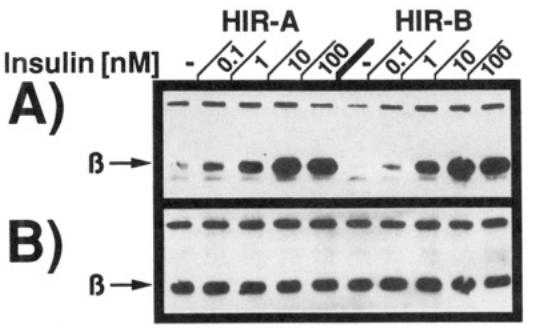

FIGURE 7: Transient expression of HIR-A and HIR-B in 293 cells. 293 cells transiently expressing either HIR-A or HIR-B were stimulated with insulin for 10 min as indicated. Cells were lysed, and receptors were immunoprecipitated with anti-receptor antibody 83-14 and analyzed by SDS–PAGE. Proteins were transferred to nitrocellulose and first blotted with anti-phosphotyrosine antibody (A) and then reblotted with the anti-receptor antibody CT104 (B).

α-subunit of the insulin receptor with ^{125}I-insulin by chemical cross-linking. Prior to cross-linking, one sample of this aliquot was trypsinized for 30 s. The second aliquot was used for autophosphorylation with [γ-^{32}P]ATP. One sample was stimulated with insulin, and a second sample was trypsinized for 30 s. The results of these experiments are shown in the autoradiograms of the upper panel of Figure 6. Both HIR-A and HIR-B show comparable amounts of α-subunit labeling (lane B: HIR-A, 1591 cpm; HIR-B, 1528 cpm). Labeling of insulin receptor α-subunit can be completely inhibited in the presence of excess unlabeled insulin (100 nM), demonstrating that ^{125}I-insulin is specifically cross-linked to the insulin receptor α-subunit (lane A). After 30 s of trypsinization, the α-subunit was cleaved and α-subunit labeling was no longer detectable on the autoradiogram (lane C). Receptor autophosphorylation after insulin stimulation is shown in lane D. Despite similar labeling of α-subunits, the ^{32}P incorporation into the β-subunit, as determined by counting of the excised band, was 2.66-fold ($\pm$0.76, n = 5) higher in HIR-B. In contrast, ^{32}P incorporation into the 80 and 60-kDa fragments of the β-subunit after trypsinization was only to a small degree higher in HIR-B (1.14-fold $\pm$ 0.62, n = 5) after 30 and 60 s. These results show that in five independent receptor preparations the ratio of labeling of the 80- and 60-kDa bands was almost equal for HIR-A and HIR-B. In contrast, the ^{32}P incorporation into the 95-kDa β-subunit was approximately 2.66-fold higher in HIR-B.

Insulin-Stimulated Autophosphorylation and Tyrosine Kinase Activation in Intact Cell. Further studies were performed to determine the kinase activity in vivo. The autophosphorylation activity was measured in embryonic human kidney fibroblasts 293 transiently overexpressing type A or type B human insulin receptor at comparable amounts. After incubation with different insulin concentrations, the cells were lysed and the solubilized proteins were analyzed by SDS–PAGE, transferred to nitrocellulose, and subjected to an immunoblot with anti-phosphotyrosine antibody. Figure 7A shows that both receptor types reveal the same dose response of their β-subunit autophosphorylation. To prove that equal receptor amounts are present, the anti-phosphotyrosine antibody was stripped off and the nitrocellulose was reblotted against an anti-β-subunit antibody (CT104). Figure 7B shows that this antibody detects equal amounts of receptor in all lanes. Therefore, intact cells which transiently overexpress the insulin receptor isotypes did not reveal the difference in tyrosine kinase activity which was detected for solubilized receptors.

When the same experimental approach (direct comparison

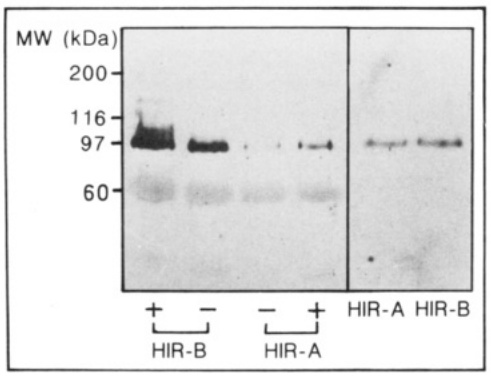

FIGURE 8: In vitro autophosphorylation of the insulin receptor. WGA-purified receptor eluate from HIR-A and HIR-B was adjusted to the same receptor amounts according to the Scatchard analysis. After stimulation with or without insulin, samples were analyzed by SDS–PAGE, and proteins were transferred to nitrocellulose and blotted with a p-tyr and a β-subunit antibody. The Figure shows the blot with the β-subunit antibody CT104 (right) and with the p-tyr antibody (left). Autophosphorylation was measured after stimulation with (+) or without (−) 100 nM insulin.

of Western blotting detection with CT104 and p-tyr antibody) was performed in vitro with solubilized receptor instead of intact cells, a clear difference of p-tyr labeling can be seen in Figure 8 [scanning densitometric analysis (total absorption): anti β-subunit CT104, HIR-A 858, HIR-B 1212; p-tyr antibody, HIR-A (basal) 503 and (100 nM insulin) 1633, HIR-B (basal) 3626 and (100 nM insulin) 6626].

To determine the in vivo kinase activity toward the substrate poly(GluNa,Tyr 4:1), we used a method described by Klein et al. (1986). HIR-A and HIR-B were stimulated with 100 nM insulin in overexpressing rat-1 fibroblasts. Insulin receptors were then prepared in the presence of phosphatase inhibitors, and the activity against poly(GluNa,Tyr 4:1) was determined as described in the Methods section. After normalization for equal insulin binding, we found a 2.9-fold (±0.54, $n = 5$) higher activity for substrate phosphorylation in HIR-B. Thus, when solubilized receptor was used, after in vivo stimulation the difference between HIR-A and HIR-B was comparable to the in vitro stimulation.

Discussion

Binding Properties of HIR-A and HIR-B. Our data confirm earlier findings that the two receptor isoforms HIR-A and HIR-B display different binding characteristics. The displacement curves of ^{125}I-insulin by unlabeled insulin confirm a previous report suggesting a higher affinity of HIR-A for insulin (Mosthaf et al., 1990). However, in our wheat germ purified preparations, this difference is less evident.

Kinase Properties of HIR-A and HIR-B in Vitro. Determination of kinase activities of both receptor types revealed a higher tyrosine kinase activity for HIR-B in vitro, but not in vivo. For a quantitative comparison of the kinase activities of these two receptor types in vitro, the reliable determination of receptor number is an essential prerequisite. To obtain as much information as possible on this point, we used different approaches to calculate phosphorylation per receptor number. We normalized ^{32}P incorporation in receptor β-subunits on the basis of receptor numbers as determined by Scatchard plots, by chemical cross-linking of ^{125}I-insulin to α-subunits, by Western blotting with antibodies against the β-subunit (CT104), and by biosynthetic labeling of receptors. All methods suggest a higher ^{32}P incorporation in HIR-B per equal amount of receptors. In addition, the experiment shown in Figure 6 where ^{32}P incorporation after trypsinization of the β-subunit was measured supported further the conclusion that same receptor amounts were used. The ratio of ^{32}P incorporation into the 80- and 60-kDa fragments correlates well with the ratio of α-subunit labeling. This provides additional evidence that increased ^{32}P incorporation in the β-subunit of HIR-B occurs.

Mechanism of Kinase Modulation. Our data suggest that the difference in kinase activity is intrinsic to the receptor and not caused by other regulatory proteins. The specific properties of HIR-A and HIR-B kinase are retained after immunoprecipitation and extensive washing of the antibody receptor immune complex. There is no evidence that loosely associated proteins with regulatory functions on receptor kinase activity, such as G-proteins, would stay associated with the insulin receptor under these conditions (Kellerer et al., 1991). However, this might not be the case with tightly associated proteins like PI-3 kinase. In contrast, one could expect that a modulation of kinase activity by serine phosphorylation would be preserved throughout the immunoprecipitation process. We could however, find no evidence for such a serine kinase activity with our receptor preparation since no ^{32}P incorporation into serine residues was detected. Alternatively, it is conceivable that prior to the purification HIR-A and HIR-B are already in a different state of serine phosphorylation in the intact cell. This possibility is unlikely for several reasons: (1) If the receptor kinase is inhibited in the intact cell by stimulation of cyclic AMP kinase or protein kinase C, this inhibition is retained during the receptor purification process only in the presence of serine phosphatase inhibitors (Häring et al., 1986a,b). In our present protocol, we did not use serine phosphatase inhibitors. (2) Furthermore, at least when cyclic AMP kinase or protein kinase C-induced serine phosphorylation has caused the inhibition of the insulin receptor kinase, we observed consistently an alteration of the K_m for ATP of the partially purified receptor (Häring et al., 1986a,b). Such an alteration of the K_m cannot be detected for HIR-A and HIR-B, which argues against a different serine phosphorylation state of HIR-A and -B as well.

Unaltered Autophosphorylation Cascade. After insulin stimulation, autophosphorylation of the insulin receptor occurs at several tyrosine residues. Approximately, 50% of the ^{32}P incorporation occurs in tyrosine residues 1146, 1150, and 1151 or 1158, 1161, and 1162, respectively (White et al., 1988). Trypsinization of the receptor β-subunit and separation of phosphopeptides by HPLC revealed five major peaks. It has been shown that three peaks represent a peptide including the neighboring tyrosine residues, while two peaks represent peptides from the C-terminal part of the insulin receptor β-subunit (White et al., 1988). The peaks pY1 and pY1a represent the triphosphorylated form of the regulatory peptide, while pY4 and pY5 represent two disphosphorylated forms. It has been shown previously that tyrosine kinase activity correlates with the amount of diphosphorylated and triphosphorylated peptide (White et al., 1988). It was suggested that the transition to a high active kinase form occurs when the triphosphorylated form is reached (White et al., 1988). There are examples that this step can be modulated (Obermaier et al., 1989). Our experiments show no major differences in tryptic peptide profiles of HIR-A and HIR-B. The relative ratio of diphosphorylated and triphosphorylated peptides under basal and insulin-stimulated conditions is similar for both receptor variants, suggesting that the intramolecular autoactivation cascade of the β-subunit does not differ in HIR-A and HIR-B subtypes.

The Kinase Difference Is Linked to the Presence of the α-Subunit. In summary, there is no evidence that the difference of the kinase activities is caused by an alteration of the β-subunit phosphorylation pattern. This conclusion is supported by the trypsin experiments shown in Figure 6. When α-subunits were cleaved by trypsin, equal amounts of receptor β-subunit phosphorylation were found. The observation that trypsinization can activate the receptor kinase (Shoelson et al., 1988) has led to the speculation that the α-subunits of insulin receptors function as inhibitors of the receptor β-subunit and its kinase activity. As similar kinase activities are found after cleavage of the α-subunits, it may be concluded that the different kinase activities in the presence of the α-subunits are caused by differences in the modulatory functions of the α-subunits. Thus, our data strongly suggest that the 12-amino-acid sequences at the C-terminal part of the HIR-B α-subunit has a crucial function for the overall conformation of the insulin receptor and may be crucial for the interaction between α- and β-subunits. Because an increased autophosphorylation of the β-subunit of HIR-B is found not only under insulin-stimulated conditions but also under basal conditions, it may be concluded that the α-subunit of HIR-A is more potent in inhibiting the kinase activity of the β-subunit than the α-subunit of HIR-B that carries the additional amino acid sequence. Thus, alternative splicing of a primary gene transcript serves as a mechanism for the modulation of both ligand binding affinity and signaling activity of the insulin receptor.

In contrast to these studies which are based on solubilized receptors the difference in autophosphorylation activity could not be detected in intact 293 cells transiently overexpressing the insulin receptor isotypes. These different results obtained after in vivo and in vitro studies could be explained in the following way: In contrast to receptors integrated into the plasma membrane of intact cells, the solubilized receptors might be able to undergo different conformational changes based on their 12-amino-acid difference in the α-subunit. These conformational changes might determine differences in the tyrosine kinase activity. This conclusion is further supported by the substrate phosphorylation studies. When substrate phosphorylation was measured after in vivo stimulation of rat-1 fibroblasts with insulin, there was also a clear difference in the tyrosine kinase activity. The experimental approach for in vivo stimulated substrate phosphorylation is completely different from the intact cell experiment based on transient expression. For poly(GluNa Tyr 4:1) phosphorylation, the insulin receptor was stimulated in vivo and substrate phosphorylation activity was measured on solubilized receptors which were prepared in the presence of phosphatase inhibitors from insulin-stimulated cells. Therefore, these in vivo stimulated insulin receptors might also be able to undergo conformational changes which determine the difference in substrate phosphorylation.

In conclusion, these data show that solubilized receptors react different from receptors integrated into the plasma membrane. The 12-amino-acid difference of the two receptor types determines different tyrosine kinase activities *in vitro*, whereas kinase activities in intact 293 cells were identical. These data show that a solubilized receptor has distinct features from a receptor integrated into the plasma membrane. At present, it is not known whether these differences of kinase activity can also occur when HIR-A and HIR-B are in their natural environment in classical target cells of insulin action. Therefore, the physiological significance of these observations and their possible relevance for the pathogenesis of type-II diabetes remain to be elucidated.

ACKNOWLEDGMENTS

We thank T. Dull (Genentech) and D. A. McClain (UCSD) for constructing the HIR-A and HIR-B expression plasmids and transfection into rat-1 cells, respectively.

REFERENCES

Braun, S., Raymond, W. E., & Racker, E. (1984) *J. Biol. Chem. 259*, 2051–2054.

Chen, C., & Okayama, H. (1987) *Mol. Cell. Biol. 7*, 2745–2752.

Ebina, Y., Ellis, L., Jarmagin, K., Edery, M., Graf, L., Clauser, E., Ou, J.-H., Masiarz, F., Kan, Y. W., Goldfine, I. D., Roth, R., & Rutter, W. (1985) *Cell 46*, 747–758.

Fendly, B. M., Winget, M., Hudziak, R. M., Lipari, M. T., Napier, M. A., & Ullrich, A. (1990) *Cancer Res. 50*, 1550–1558.

Gorman, C. M., Gies, D., McCray, G., & Huang, M. (1989) *Virology 171*, 377–385.

Häring, H. U., Kasuga, M., White, M. F., Crettaz, M., & Kahn, C. R. (1984) *Biochemistry 23*, 3298–3306.

Häring, H. U., Kirsch, D., Obermaier, B., Ermel, B., & Machicao, F. (1986a) *Biochem. J. 234*, 59–66.

Häring, H. U., Kirsch, D., Obermaier, B., Ermel, B., & Machicao, F. (1986b) *J. Biol. Chem. 261*, 3869–3875.

Häring, H. U., White, M. F., Machicao, F., Ermel, B., Schleicher, E., & Obermaier, B. (1987) *Proc. Natl. Acad. Sci. U.S.A. 84*, 113–117.

Kahn, C. R., White, M. F., Grigorescu, F., Häring, H. U., & Crettaz, M. (1985) *Molecular Basis of Insulin Action* (Czech, M., Ed.) pp 67–93, Plenum Press, New York.

Kasuga, M., Van Obberghen, E., Nissley, S. P., & Rechler, M. M. (1981) *J. Biol. Chem. 256*, 5305–5308.

Kasuga, M., Zick, Y., Blithe, D. L., Karlsson, F. A., Häring, H. U., & Kahn, C. R. (1982) *J. Biol. Chem. 257*, 9891–9894.

Kellerer, M., Obermaier-Kusser, B., Prüfrock, A., Schleicher, E., Mushack, J., Seffer, E., Ermel, B., & Häring, H. U. (1991) *Biochem. J. 276*, 103–108.

Klein, H., Freidensberg, G. R., Kladde, M., & Olefsky, J. M. (1986) *J. Biol. Chem. 261*, 4691–4697.

McPherson, G. A. (1985) *J. Pharmacol. Methods 14*, 213–218.

Mosthaf, L., Grako, K., Dull, T. J., Coussens, L., Ullrich, A., & McClain, D. A. (1990) *EMBO J. 9*, 2409–2413.

Obermaier, B., White, M. F., Pongratz, D., Su, Z., Ermel, B., Mühlbacher, Ch., & Häring, H. U. (1989) *J. Biol. Chem. 245*, 9497–9504.

Pilch, P. F., & Czech, M. P. (1979) *J. Biol. Chem. 254*, 3375–3381.

Roth, R. A., Morgan, D. O., Beaudoin, J., & Sara, V. (1986) *J. Biol. Chem. 261*, 3753–3757.

Seino, S., & Bell, F. I. (1989) *Biochem. Biophys. Res. Commun. 159*, 312–316.

Shoelson, S. E., White, M. F., & Kahn, C. R. (1988) *J. Biol. Chem. 263*, 4852–48–60.

Soos, M. A., Siddle, K., Baron, M. D., Heward, J. M., Luzio, J. P., Bellatin, J., & Lennox, E. S. (1986) *Biochem. J. 235*, 199–208.

Ullrich, A., Bell, J. B., Chen, E. Y., Herrera, R., Petruzelli, L. L. M., Dull, T. J., Gray, A., Coussens, L., Liao, Y.-C., Tsubokawa, M., Mason, A., Seeburg, P. H., Grunfeld, C., Rosen, O. M., & Ramachandran, J. (1985) *Nature 313*, 756–761.

Van Wyk, J. J., Svoboda, M. E., & Underwood, L. E. (1980) *J. Clin. Endocrinol. Metab. 50*, 206-208.
White, M. F., Häring, H. U., Kasuga, M., & Kahn, C. R. (1984) *J. Biol. Chem. 259*, 255-264.
White, M. F., Maron, R., & Kahn, C. R. (1985) *Nature 318*, 183-186.
White, M. F., Shoelson, S. E., Keutmann, H., & Kahn, R. (1988) *J. Biol. Chem. 263*, 2969-2980.
Williams, P. F., & Turtle, J. R. (1979) *Biochim. Biophys. Acta 579*, 367-374.
Yarden, Y., & Ullrich, A. (1988) *Annu. Rev. Biochem. 57*, 443-47.

X-ray Absorption Spectroscopic Studies of the High-Spin Iron(II) Active Site of Isopenicillin N Synthase: Evidence for Fe–S Interaction in the Enzyme–Substrate Complex†

Robert A. Scott,* Shengke Wang, and Marly K. Eidsness

Departments of Chemistry and Biochemistry and Center for Metalloenzyme Studies, University of Georgia, Athens, Georgia 30602

Aidas Kriauciunas, Charles A. Frolik, and Victor J. Chen*

Lilly Research Laboratories, Indianapolis, Indiana 46285

Received December 18, 1991; Revised Manuscript Received February 28, 1992

ABSTRACT: Isopenicillin N synthase from *Cephalosporium acremonium* (IPNS; M_r 38.4K) is an Fe^{2+}-requiring enzyme which catalyzes the oxidative conversion of (L-α-amino-δ-adipoyl)-L-cysteinyl-D-valine (ACV) to isopenicillin N, with concomitant reduction of O_2 to $2H_2O$. Chemical and spectroscopic data have suggested that catalysis proceeds via an enzyme complex of ACV bound to the iron through its cysteinyl thiolate [Baldwin, J. E., & Abraham, E. P. (1988) *Nat. Prod. Rep. 5*, 129-145; Chen, V. J., Orville, A. M., Harpel, M. R., Frolik, C. A., Surerus, K. K., Münck, E., & Lipscomb, J. D. (1989) *J. Biol. Chem. 264*, 21677-21681; Ming, L.-J., Que, L., Jr., Kriauciunas, A., Frolik, C. A., & Chen, V. J. (1991) *Biochemistry 30*, 11653-11659]. Here we have employed the technique of Fe K-edge extended X-ray absorption fine structure (EXAFS) to characterize the iron site and to seek direct evidence for or against the formation of an Fe–S interaction upon ACV binding. Our data collected in the absence of substrate and O_2 are consistent with the iron center of IPNS being coordinated by only (N,O)-containing ligands in an approximately octahedral arrangement and with an average Fe–(N,O) distance of 2.15 ± 0.02 Å. Upon anaerobic binding of ACV, the iron coordination environment changes considerably, and the associated Fe EXAFS cannot be adequately simulated without incorporating an Fe–S interaction at 2.34 ± 0.02 Å along with four or five Fe–(N,O) interactions at 2.15 ± 0.02 Å. Although these data cannot rule out incorporation of an endogenous thiolate from the protein coincident with ACV binding, evidence presented in the following paper indicates that the thiolate ligand originates from ACV [Orville, A. M., Chen, V. J., Kriauciunas, A., Harpel, M. R., Fox, B. G., Münck, E., & Lipscomb, J. D. (1992) *Biochemistry* (following paper in this issue)]. Multiple-scattering analysis of the EXAFS data shows that two or three of the Fe–(N,O) interactions are likely due to histidyl imidazole ligation, both in the presence and in the absence of ACV.

Isopenicillin N synthase (IPNS;[1] M_r 38.4K) is a mononuclear Fe^{2+}-dependent enzyme (Chen et al., 1989) which catalyzes the formation of isopenicillin N from (L-α-amino-δ-adipoyl)-L-cysteinyl-D-valine (ACV); concomitantly, one O_2 is reduced to $2H_2O$ (White et al., 1982; Baldwin & Abraham, 1988; Scheme I), in classic oxidase stoichiometry. To date, IPNS is the only oxidase known among a growing number of mononuclear non-heme Fe^{2+}-dependent enzymes. More typically, the enzymes in this class catalyze oxygenase chemistry, wherein one or both atoms of O_2 are incorporated into substrates (Ingraham & Meyer, 1985). A variety of activation mechanisms have been proposed for these enzymes, all invoking activation of O_2 through interaction with the enzyme-bound iron center.

The roles of O_2 and iron in the IPNS reaction are less well-defined. Since the double ring closure of ACV is a 4-electron oxidation process, O_2 may serve as an electron acceptor analogous to its role in cytochrome *c* oxidase (Chan et al., 1988). Alternatively, O_2 may be activated at the iron center to become a reagent which is essential for generating certain reactive substrate intermediates during the ring closure reaction. Pursuant to this hypothesis is a mechanism for IPNS

† XAS studies at the University of Georgia are supported by National Institutes of Health Grant GM-42025 to R.A.S.

* Correspondence can be addressed to either of these authors. The address for V.J.C. is Lilly Research Laboratories, MC797, Lilly Corporate Center, Indianapolis, IN 46285.

[1] Abbreviations: ACV, (L-α-amino-δ-adipoyl)-L-cysteinyl-D-valine; EXAFS, extended X-ray absorption fine structure; IPNS, isopenicillin N synthase; MOPS, 3-(*N*-morpholino)propanesulfonic acid; XAS, X-ray absorption spectroscopy.

0006-2960/92/0431-4596$03.00/0